

Evaluation of the generalization performance of a CNN-assisted BOFDA system

Christos Karapanagiotis, Bundesanstalt für Materialforschung und -prüfung (BAM), Unter den Eichen 87, Berlin, Germany

Abstract

Brillouin Optical Frequency Domain Analysis (BOFDA) is a powerful and well-established method for static distributed sensing of temperature and strain. Recently, we demonstrated a BOFDA system based on convolutional neural network which shortens the measurement time considerably. In this paper, we apply leave-one-out cross validation to evaluate the generalization performance and provide an unbiased and reliable machine learning model for a time-efficient BOFDA system.

1 Introduction

Over the last few years, machine learning and artificial neural networks (ANN) in particular, have been used in the field of distributed fiber optic sensors (DFOS) to enhance their performance, extract insights of the raw data, decouple multiple measurands, denoise spectra and reduce the measurement time [1-4]. Recently, we published an approach based on ANN and specifically convolutional neural networks (CNN) to enhance the performance of a Brillouin Optical Frequency Domain Analysis (BOFDA) sensor in terms of measurement time [3].

BOFDA is among the well-established sensing techniques in DFOS providing high spatially resolved distributed information (even on cm scale) of temperature or strain along ultra-long (up to 100 km) distances [5, 6]. This renders BOFDA appropriate sensing solution for a wide range of applications from structural health monitoring of infrastructures like bridges, dams, river embankments to long pipeline and subsea cables monitoring. BOFDA sensing is characterized by the narrow measurement bandwidth which on the one hand provides high signal-to-noise ratio and reduces the total cost (since no fast electronics are needed) but on the other hand increases significantly the measurement time. Our proposed CNN-assisted BOFDA reduced the measurement time by more than nine times [3].

ANNs and CNNs are very powerful algorithms but in comparison to conventional algorithms they are very prone to overfitting and thus the algorithm's hyperparameters have to be optimized and cross validation methods have to be employed in order to estimate the model's uncertainties. Unfortunately, error estimation of such algorithms is not trivial and long training times are expected.

In this paper we demonstrate a reliable and unbiased approach for error estimation in our newly developed CNN-assisted BOFDA system and we evaluate the ability of the algorithm to not only generalize but also to interpolate on

new data. To this end, we make use of leave-one-out cross validation (LOOCV) approaches [7].

2 Methods

2.1 Experimental setup and data acquisition

BOFDA is based on the inelastic scattering between continuous pump waves and the acoustic waves (acoustic phonons) in the medium. The resulted backscattered wave has a frequency equal to the frequency of the pump and the acoustic wave. The frequency of the acoustic phonons is characteristic of the medium and is equal to the so-called Brillouin frequency shift (BFS). Because the backscattered signal is weak, a counter-propagate probe (Stokes) wave is injected from the other end of the fiber under test (FUT) to stimulate the effect. Both probe and

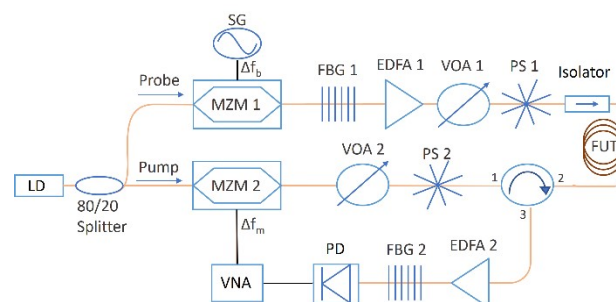


Figure 1. BOFDA experimental setup. LD: laser diode; MZM: Mach-Zehnder modulator; SG: signal generator; FBG: fiber Bragg grating; EDFA: erbium-doped fiber amplifier; VOA: variable optical attenuator; PS: polarization scrambler; FUT: fiber under test; PD: photodiode; VNA: vector network analyzer.

(LD) which emits at 1550 nm. The LD is followed by an 80/20 fiber splitter. The probe path tunes the BFS so that stimulated emission occurs. To this end, a Mach-Zehnder modulator (MZM 1) and a signal generator (SG) that works in GHz range are employed to suppress the carrier and generate two sidebands, where only the upper one

passes through the fiber Bragg grating filter. In the pump path, the signal's amplitude is modulated in a frequency range from f_{min} to f_{max} with a step $\Delta f_m = f_{min} \cdot \Delta f_m$ and f_{max} determine the measurement length and the spatial resolution, respectively. In this paper the measurement length is more than 30 km and the spatial resolution is 25 m. The polarization scramblers (PS) are employed to reduce the polarization fading. The isolator in the probe path protects the optical components from the transmitted pump signal. The backscattered signal from the FUT ends up through a circulator, an erbium-doped fiber amplifiers (EDFA) and second FBG (FBG 2) to a photodiode (PD), which transforms the optical signal into electrical signal. The FBG 2 is used to filter out the backscattered Rayleigh component. The VNA records the systems response $H(j\omega, \Delta f_m)$, can be transferred to time domain via inverse fast Fourier transformations (iFFT) and then converted into spatial resolved BGS as follows :

$$H(j\omega, \Delta f_m) \xrightarrow{iFFT} h(t, \Delta f_m) \xrightarrow{z=\frac{1c}{2n}t} h(z, \Delta f_m)$$

Before iFFT, zero padding can be applied to the system's response to increase the Nyquist frequency and thus the spatial sampling [8]. In this paper we increased the Nyquist frequency by 16 times and thus 16 BGS correspond to the defined spatial resolution.

2.2 The CNN-based approach

An illustrative comparison of the conventional method and the CNN approach to acquire distributed temperature information from the raw data is shown in Figure 2. Conventionally with BOFDA, the temperature is estimated by the so-called BFS that is obtained by employing Lorentzian curve fitting (LCF) to the BGS. The CNN-assisted BOFDA extracts spatial information of temperature directly from the BGS without the need of any least-square fitting algorithm. The performance of the LCF algorithm is affected by the signal-to-noise ratio (SNR) and the Brillouin frequency scan points. A characteristic LCF fitting is depicted in Figure 2a. LCF has to be performed under different temperature conditions in order to retrieve the temperature coefficient of the FUT via linear fitting. We note that the temperature extracted from every 16 BGS (corresponding to the defined spatial resolution) is averaged.

The architecture of the CNN-assisted BOFDA is shown in Figure 2b. Its input consists of 16 BGS (within the defined spatial resolution) while its output is a single value of temperature. The network's architecture is similar to the VGG16 that is usually used for image recognition [9].

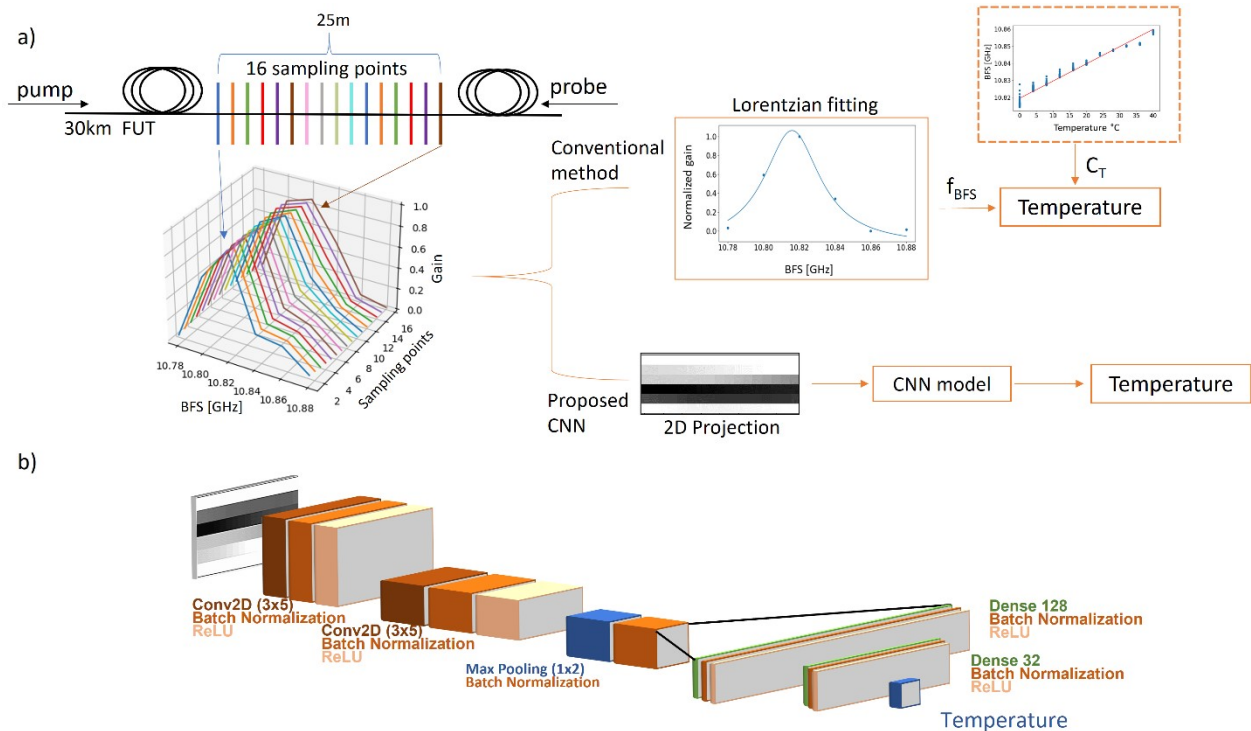


Figure 2. a) Illustrative comparison between the conventional and the convolutional neural network (CNN)-based method. b) CNN architecture. The input consists of a 6×16 (Brillouin frequency steps \times number of BGS) spectrum while the output is a single value for temperature. Convolutional layers employ 3×5 filters with a depth of 16 and 32 for the first and second layers, respectively. After flattening, two fully connected (FC) layers are used. Batch normalization and ReLU activation functions follow every convolutional and FC layer [3].

2.3 Data acquisition and error estimation

The measurements are carried out using a temperature chamber, in which an optical fiber segment of 200 m is placed. This segment is connected to the 30-km fiber loop, and we call it fiber-under-test (FUT). We conduct measurements in two ways. First, we place the FUT before the 30-km fiber loop and then after it. This results in BGS with high and low SNR since at the end of the 30-km fiber loop the SNR is reduced significantly. The measurements are conducted at set temperatures from 0 °C to 40 °C with a step of 4 °C. At every temperature, 20 distributed temperature measurements along the whole optical fiber are conducted in total. We note that even though we measure along the whole optical fiber only the data from the FUT are used in this paper. After the collection of data, data augmented methods such as horizontal flipping are applied.

Error estimation is of great importance in machine learning to ensure that the models are reliable and generalize well. In this paper, we make use of LOOCV, which is an iterative method to estimate the model's performance by using each observation for testing and the rest for training [7]. The number of iterations is equal to the number of observations. As observation we consider either a single measurement along the optical fiber or all the measurements corresponding to the same temperature. For the sake of simplicity, we call these methods leave-one-measurement-out cross validation (LOMOCV) and leave-one-temperature-out cross validation (LOTOCV), respectively. The LOMOCV provides an estimation of the model to generalize on data out of the training set while LOTOCV additionally shows the interpolation ability of the model.

3 Results and discussion

In this paper, we train CNNs with the hyperparameters that are used in [3]. Specifically, the number of epochs is 100, the batch size is 64 and the learning rate is set to 0.001. The hyperparameters regarding the structure of the CNN are shown in Figure 2. Furthermore, the CNNs are trained using the Keras library (v. 2.3.1) [10] and an NVIDIA GeForce RTX 2080 Ti 11GB RAM GPU.

As we mentioned in the previous section, the FUT is placed at the beginning and at the end of a 30-km fiber loop. In Figure 3 we make use of LOTOCV and LOMOCV to estimate the system's performance in terms of MAE including a) the whole dataset, b) only data from the FUT placed at the beginning of the fiber loop and c) only data from the FUT placed at the end of the 30-km fiber loop. The green boxes correspond to the CNN model while the orange ones to the conventional methods based on LCF. The boxplots are described by the boxes and the whiskers. The boundaries of the boxes define the inter-quartile range with the horizontal line within the box representing the median value. The boundaries of the lower

and upper whiskers show the minimum and the maximum value. The white dots represent the mean error.

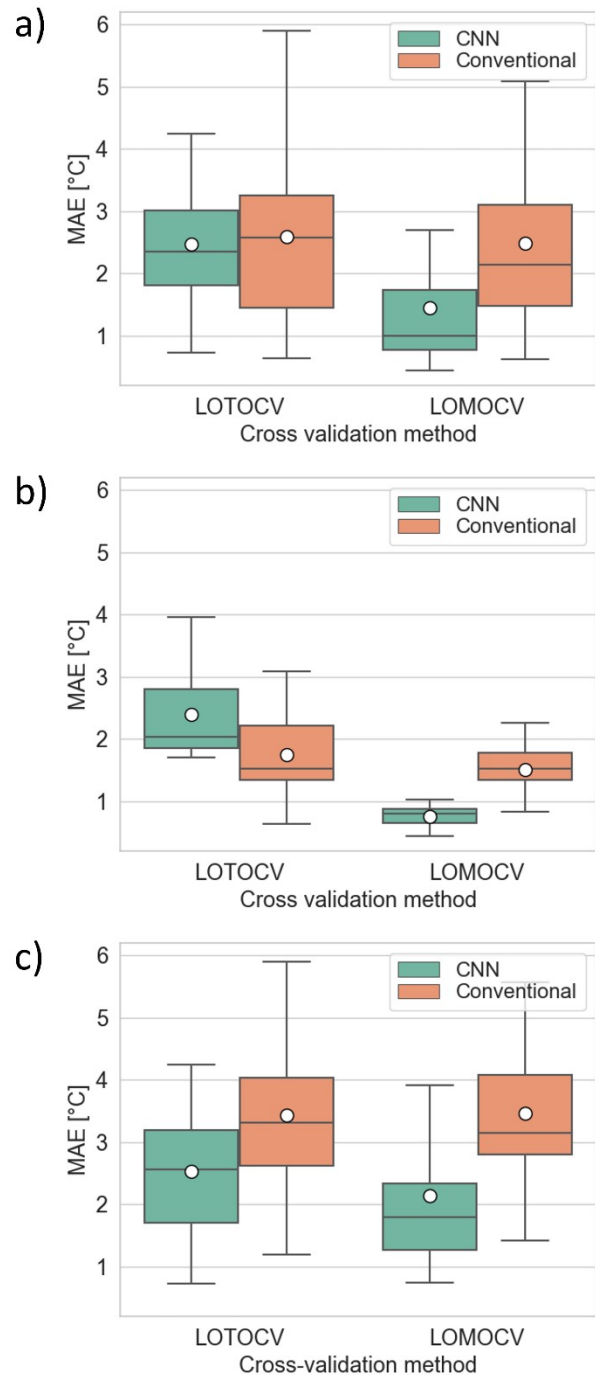


Figure 3: MAE estimated by applying LOTOCV and LOMOCV on a) the whole dataset, b) only on data from the FUT placed at the beginning of the fiber loop and c) only on data from the FUT placed at the end of the fiber loop.

In Figure 3a, where all the data are included, we observe that the CNN performs better than the conventional algorithm in any cross validation case with the former performing considerably better when the labels of the test data are also included in the training set (LOMOCV). In both cases, the CNN model results in a lower error deviation. In contrast to the CNN approach, the LOTOCV and LOMOCV of the conventional method do not result in

significantly different MAE. This is attributed to the simplicity of the conventional model, which assumes only linear relations and has inherently low variance.

Figure 3b shows the MAE from the data collected from the FUT placed at the beginning of the 30-km fiber loop. We observe that while the MAE of the CNN model is lower than the conventional model when LOMOCV is employed, this is not the case when LOTOCV is used. In Figure 3c only the MAE from the data collected when the FUT is placed at the end of the fiber loop, is shown. In this case the CNN outperforms the conventional algorithm with the error difference between the two models being higher when LOMOCV is employed. Nevertheless, the CNN interpolation ability (LOTOCV) is significantly higher than that of the conventional method by almost 1 °C. Furthermore, the error deviation is lower when CNNs are used.

In all plots of Figure 3, we observe that the LOTOCV approach results in higher errors than the LOMOCV. This is expected since the algorithm does not only need to generalize on new data but to interpolate. The performance of the CNN model could be further improved by enhancing the temperature resolution in the training set.

Our results show that the CNN model performs considerably better on data with low SNR than the conventional method. In BOFDA, the SNR decreases with the sensing distance and thus the tolerance against noise of the CNNs is of high importance showing the potential to extend the measurement length without additional components. Furthermore, the SNR depends strongly on the measurement time. A high SNR is achieved by narrowing the measurement bandwidth and increasing the number of averages in the VNA, which both result in longer measurements. So as we already have shown in [3] the CNN shortens the measurement time considerably due to its great noise-tolerance.

4 Conclusions

In this paper, we evaluated the generalization performance of a CNN-assisted BOFDA, and we conclude that the CNN approach performs significantly better on data with low SNR. Our error estimation approach showed that the CNN model not only generalizes but also interpolates better than the conventional approach. Our results verify that the reported CNN-assisted BOFDA paves the way towards new applications for BOFDA (e.g. long pipeline and subsea cable monitoring), where faster measurement time is essential.

5 Acknowledgments

CK acknowledges the financial support by the PhD-program of Bundesanstalt für Materialforschung und -prüfung (BAM)

6 Literature

- [1] S. Liehr, "Artificial neural networks for distributed optical fiber sensing (Invited)," in *2021 Optical Fiber Communications Conference and Exhibition (OFC)*, 2021, pp. 1-4.
- [2] S. Liehr, L. A. Jäger, C. Karapanagiotis, S. Münzenberger, and S. Kowarik, "Real-time dynamic strain sensing in optical fibers using artificial neural networks," *Opt. Express*, vol. 27, no. 5, pp. 7405-7425, 2019.
- [3] C. Karapanagiotis, A. Wosniok, K. Hicke, and K. Krebber, "Time-Efficient Convolutional Neural Network-Assisted Brillouin Optical Frequency Domain Analysis," *Sensors (Basel)*, vol. 21, no. 8, 2021.
- [4] A. Venkateswaran *et al.*, "Recent Advances in Machine Learning for Fiber Optic Sensor Applications," *Advanced Intelligent Systems*, vol. 4, no. 1, 2022
- [5] T. Kapa, A. Schreier, and K. Krebber, "A 100-km BOFDA Assisted by First-Order Bi-Directional Raman Amplification," (in English), *Sensors-Basel*, vol. 19, no. 7, 2019
- [6] R. Bernini, A. Minardo, and L. Zeni, "Distributed Sensing at Centimeter-Scale Spatial Resolution by BOFDA: Measurements and Signal Processing," *IEEE Photonics Journal*, vol. 4, pp. 48-56, 2012
- [7] Y. L. Zhang and Y. H. Yang, "Cross-validation for selecting a model selection procedure," (in English), *J Econometrics*, vol. 187, no. 1, pp. 95-112, 2015
- [8] R. G. Lyons, Understanding digital signal processing, Prentice Hall/PTR: Upper Saddle River, NJ, USA, 2004.
- [9] K. Simonyan and A. Zisserman, "Very deep convolutional networks for large-scale image recognition," *arXiv preprint arXiv:1409.1556*, 2014.
- [10] F. Chollet, "Keras: The python deep learning library," GitHub Inc.: San Francisco, CA, USA, 2015